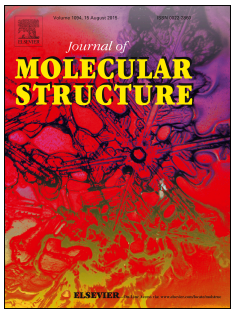

Synthesis and photophysical properties of monomeric and dimeric halogenated aza-BODIPYs

H. Şeyma Çınar, Şennur Özçelik, Kerem Kaya, Öznur Dülger Kutlu, Ali Erdoğmuş, Ahmet Gül

PII: S0022-2860(19)31214-1

DOI: https://doi.org/10.1016/j.molstruc.2019.127108

Reference: MOLSTR 127108

To appear in: *Journal of Molecular Structure*

Received Date: 3 July 2019

Revised Date: 17 September 2019

Accepted Date: 20 September 2019

Please cite this article as: H.Ş. Çınar, Ş. Özçelik, K. Kaya, Ö.Dü. Kutlu, A. Erdoğmuş, A. Gül, Synthesis and photophysical properties of monomeric and dimeric halogenated aza-BODIPYs, *Journal of Molecular Structure* (2019), doi: https://doi.org/10.1016/j.molstruc.2019.127108.

Graphical Abstract

Synthesis and Photophysical Properties of Monomeric and Dimeric Halogenated Aza-BODIPYs

H. Şeyma Çınar, Şennur Özçelik, Kerem Kaya, Öznur Dülger Kutlu, Ali Erdoğmuş, Ahmet Gül

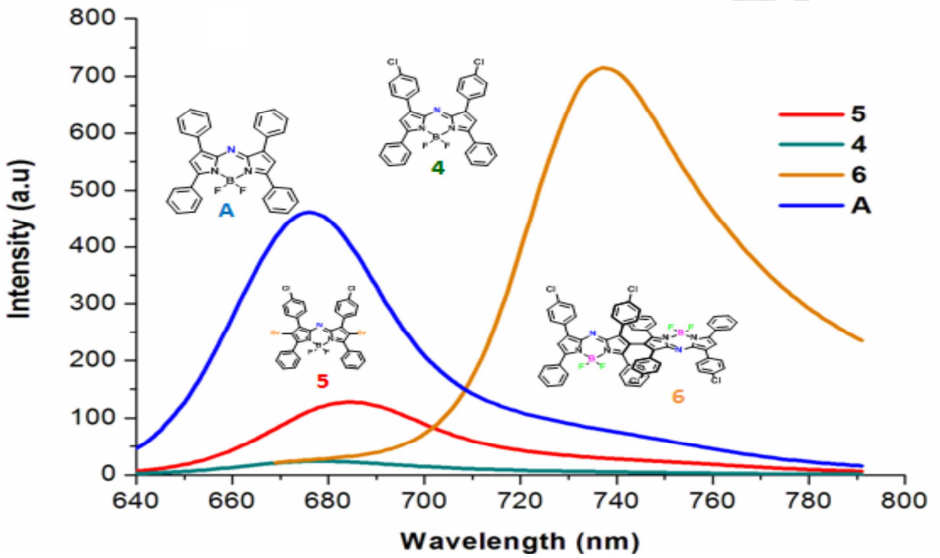

Photophysical properties of dimeric and halogenated aza-BODIPYs were investigated and compared with tetra-phenyl aza-BODIPY. The aza-BODIPY derivative carrying bromine atoms at the central core showed the highest efficiency of singlet oxygen generation.

Synthesis and Photophysical Properties of Monomeric and Dimeric Halogenated Aza-BODIPYs

H. Şeyma Çınar[a], Şennur Özçelik*[a], Kerem Kaya[a], Öznur Dülger Kutlu[b], Ali Erdoğmuş[b], Ahmet Gül*[a]

[a] Department of Chemistry, Istanbul Technical University, Maslak, Istanbul, 34469, Turkey

[b] Department of Chemistry, Yildiz Technical University, Davutpasa, Istanbul, 34210, Turkey

* Corresponding author.

E-mail address: ahmetg@itu.edu.tr; oksuzse@itu.edu.tr (A. Gül; Ş. Özçelik)

Abstract: In this study, the effects of incorporation of halogen atoms at different positions and dimerization on the photophysical properties of the aza-BODIPYs were investigated. Aza-BODIPY derivative carrying chlorine atoms on the para-position of the distal phenyl groups (**4**) and its core-brominated analogue (**5**) were prepared to establish the external and internal heavy atom effects. Dimerization of aza-BODIPY **4** through oxidative homocoupling with $FeCl_3$ yielded the target homonuclear aza-BODIPY dimer (**6**). All of the aza-BODIPY derivatives prepared in this study were fully characterized by using UV-Vis, Fluorescence, NMR (^{1}H, ^{13}C, ^{11}B and ^{19}F), Mass and X-Ray spectroscopy techniques. The photophysical properties were fully characterized and compared to those of the tetra-phenyl aza-BODIPY derivative (**A**). Singlet oxygen generation experiments were also performed. The aza-BODIPY derivative possessing bromine atoms at the central core displayed the utmost efficiency for singlet oxygen generation.

Keywords: Aza-BODIPY; photophysics; singlet oxygen generation; PDT; bromination

1. Introduction

Photodynamic therapy (PDT), noninvasive method for treatment of superficial tumors, is being recognized as an alternative to the conventional cancer therapies. This technique is consisted of two simple procedures; transferring of photosensitizing agent into the tumor and activating the sensitizer by illuminating the tumor with light of the appropriate wavelength. Upon absorption of the light, photosensitizer is light-activated from its ground state into excited singlet state. In order to obtain photodynamic effect, the photosensitizer of minimum dark toxicity should undergo electron spin conversion from its excited singlet state to triplet state. Singlet oxygen, the damaging specie in PDT, is generated by the energy transfer from excited triplet photosensitizer to molecular oxygen. This spin-forbidden transition at

photosensitizer, called as inter system crossing (ISC), has a crucial role on the effectiveness of PDT as the amount of singlet oxygen generated in this method depends directly on ISC step [1-3]. ISC is commonly enhanced by spin-orbit perturbations due to the presence of heavy atom [3] on either the absorbing core of the molecule (internal heavy atom effect) [4] or on the peripheral positions of the structure (external heavy atom effect**)** [4-6]**.**

Porphyrins, chlorins, and bacteriochlorins, most widely clinically used PDT sensitizers, are cyclic tetrapyrroles [7, 8]. These agents have some compelling drawbacks such as toilsome preparations, troubles in purification and challenging modifications for the optimization of their photophysical properties [9].

Over the last ten years, a novel PDT photosensitizer class that structurally based on dipyrromethene (DPM) and azadipyrromethene (ADPM) chromophors has emerged. DPM and ADPM can be considered structurally as half of porphyrin and porphyrazine, respectively. These bidentate ligands have attracted much attention for their photophysical properties comparable to those of porphyrinoids. Furthermore these ligands have many synthetic advantages over porphyrins; they keep away from low-yield macrocyclization step and burdensome purification processes. Moreover, bidentate motif allows these ligands to display an enormous versatility of metal coordination geometries in comparison to the rigid square-planar geometry of cyclic tetrapyrroles [10]. The most studied compounds of these chromophors are the 4,4-difluoro-4-bora-3*a*,4*a*-diaza-*s*-indacenes, BODIPYs. BODIPYs can be considered as candidates for ideal photosensitizers owing to their advantegous features such as their strong absorption in the range of 500-600 nm with high molar absorption coefficients, emission in the NIR region, moderate to high fluorescence quantum yields, and high photostability [1, 9, 11-15]. Due to these significant properties, the number of the researches on BODIPY derivatives for various applications has increased recently [3, 16-20].

The deep penetration into the tissue, an obligatory for an efficient photosensitizer, can be achieved by strong absorptions and emissions in the low energy regions (650–900 nm) [1, 21, 22]. So, numerous chemical modifications have been applied to extend their absorptions to longer wavelengths. One of the under-examined strategy is replacement of the methine group at the 8-position of the core unit with nitrogen yielding a new class of compounds, azadipyrromethenes boron difluoride (known as as aza BODIPY) [23]. The presence of nitrogen atom rather than carbon in aza-BODIPY structure causes significant photophysical properties by lowering the HOMO-LUMO energy gap [24]. Aza-BODIPYs' absorption and emission wavelengths are red-shifted for about 100 nm when compared to those of BODIPYs [25-29]. As the nitrogen atom decreases the S1−T1 energy gap by restricting the spatial overlapping between the HOMO and LUMO, the population of triplet states may be increased in aza-BODIPYs in contrast to the conventional BODIPYs [30]. Furthermore, aza-BODIPYs' molar absorption coefficients are much higher than those of porphyrins [9]. These superior photophysical properties of aza- BODIPY facilitate an efficient singlet-oxygen generation. Consequently, aza-BODIPY agents have a higher chance to be evaluated in clinical treatment than any other derivatives of BODIPY class [9, 31, 32].

Aza-BODIPYs' ability for singlet oxygen generation can be improved by the help of heavy atom effect; either by attaching halogen atoms to the core or to the peripheral phenyl rings [1, 33]. It is reported in the literature that ISC mechanism is only affected by the number of heavy atoms at the 2,6 positions of the BODIPY core [4, 34], as the heavy atoms at 2,6-position of aza-BODIPY core increase the probability of ISC due to internal heavy atom effect [35]. This internal heavy atom effect was examined by the studies conducted on their fluorescence and phosphorescence properties as well as on their ability to generate singlet oxygen of aza-BODIPY [4, 12, 34, 36, 37]. On the other hand, in the case of aza-BODIPY derivative carrying

bromine atom as a substituent on the phenyl groups, no remarkable decrease in the quantum yield was monitored [36, 38].

Dimerization leading photoinduced electron transfer (PET) can be the other chemical modification to achieve an adequate triplet state generation [39]. The number of the studies on dimeric aza-BODIPY derivatives is so limited in the literature. These papers are reporting on dimeric structures are pyrrolopyrro aza-BODIPYs (PPAB) [40-42] benzodipurrolidone-based dimeric aza-BODIPYs [43] and isoindigo-based dimeric aza-BODIPYs [44]. There is only one paper reporting on the preparation of aza-BODIPY dimer through oxidative homocoupling with $FeCl_3$ [45]. Photophysical measurements in this paper revealed that absorption maxima of the dimers were shifted to longer wavelengths when compared to the corresponding monomers [44].

In this study, it is aimed to investigate the influence of incorporation of halogen atoms and dimerization on the photophysical and photochemical properties of aza-BODIPY derivatives as well as on their efficiencies of singlet oxygen generation for their potential use as photosensitizers for photodynamic therapy. In line with this purpose, aza-BODIPY that is substituted with Cl atoms at the para position of the distal phenyl groups and its 2,6-dibrominated analogue were synthesized for elucidating the effect of halogen atoms at different positions in the aza-BODIPY system. Dimerization of the aza-BODIPY bearing chlorine atoms at distal phenyl rings was accomplished by oxidative homo-coupling with $FeCl_3$. All of the compounds were fully characterized and their photophysicochemical properties, including fluorescence behavior and their efficiencies for singlet oxygen generation were examined in THF.

2. Experimental Section

2.1. General techniques

Perkin Elmer Spectrum One FT-IR spectrometer and Scinco S-3100 spectrophotometer with a 1 cm and 1 mm path length cuvette were used to obtain the IR and UV-Vis spectra of the compounds, respectively. ^{1}H (500 MHz), ^{13}C (126 MHz), ^{11}B (160 MHz), and ^{19}F (470 MHz) NMR spectra of the compounds were recorded on Agilent VNMRS 500 MHz spectrometer. Tetramethylsilane (TMS) for ^{1}H and ^{13}C NMR, CF_4 for ^{19}F NMR and $BF_3 \cdot Et_2O$ for ^{11}B NMR were used as references. Fluorescence excitation and emission measurements were conducted on a Varian Eclipse spectrofluorometer using a 1 cm path length cuvette at room temperature. Mass results were obtained by Bruker Daltonics. X-Ray analysis was realized by Bruker D8 Venture. Melting points of the compounds were recorded on Büchi Melting Point B-540. Fluorescence-quenching experiments were performed with blended films of P3HT/M*x*L*y* in a 1:1 (wt/wt) ratio in HPLC-grade chloroform (400 μL).

2.2. Quantification of singlet oxygen generation

Photo-irradiation was done by using a General Electric quartz line lamp (300W). A 600 nm glass cut off filter (Schott) and a water filter was used to filter off ultraviolet and infrared radiations respectively. An interference filter (Intor, 670 nm or 700 nm with a bandwidth of 40 nm) was additionally placed in the light path before the sample. Light intensities were measured with a POWER MAX5100 (Molelectron detector incorporated) power meter.

2.3. Materials

4-chlorobenzaldehyde, acetophenone, ethanol (EtOH), sodium hydroxide (NaOH), nitromethane, diethylamine, 1 N hydrochloric acid (HCl), ammonium acetate, *n*-butanol, *N*,*N*-

diisopropylethylamine, boron trifluoride diethyl etherate, dichloromethane (DCM), *n*-hexane, *n*-pentane, chloroform ($CHCl_3$), petroleum ether, bromine, ethyl acetate, and iron(III) chloride were of reagent grade quality obtained from commercial suppliers. Tetra-phenyl derivative (**A**) was prepared according to the reported procedure [45, 46].

2.4. Synthesis of 3-(4-chlorophenyl)-1-phenylprop-2-en-1-one (1) [47]

A solution of 4-chlorobenzaldehyde (5.60 g, 39.0 mmol) and acetophenone (4.78 g, 4.64 mL, 39.0 mmol) in ethanol was cooled down to 0°C. A solution of NaOH (4.80 g, 120 mmol) in 100 mL of ethanol/water mixture (1:1, v/v) was added dropwise. The reaction mixture was stirred at room temperature for 24 h. The resulting off-white product was filtered, washed with cold water and cold ethanol, and dried at room temperature, yield: 7.55 g, (76%). m.p. 106–109 °C. ^{1}H NMR (500 MHz, $CDCl_3$): δ = 8.01 (d, *J* = 7.2 Hz, 2H), 7.76 (d, *J* = 16 Hz, 1H), 7.62 – 7.55 (m, 3H), 7.54 – 7.48 (m, 3H), 7.39 (d, *J* = 8.4 Hz, 2H) ppm. IR (KBr): ῡ 3059 (w, Ar-CH), 1655 (s, C=O), 1603 (m, Ar-C=C), 686 (s, C-Cl) cm-1

2.5. Synthesis of 3-(4-chlorophenyl)-4-nitro-1-phenylbutan-1-one (2) [47]

To a solution of compound **1** (2.00 g, 8.24 mmol) and diethylamine (4.30 mL, 41.2 mmol) in ethanol (45 mL) was added nitromethane (3.00 mL, 49.5 mmol) and the mixture was heated at reflux for 48 h. The reaction mixture was cooled to room temperature and quenched with 1 N HCl (10 mL). The resulting precipitate was isolated by filtration, washed with cold water and ethanol, and dried at room temperature, yield: 2.11 g, (84%). m.p. 88 °C. ^{1}H NMR (500 MHz, $CDCl_3$): δ = 7.91 (d, *J* = 7.8 Hz, 2H), 7.58 (t, *J* = 7.5 Hz, 1H), 7.46 (dd, *J* = 7.8, 7.5 Hz, 2H), 7.31 (d, *J* = 8.2 Hz, 2H), 7.23 (d, *J* = 8.2 Hz, 2H), 4.81 (dd, *J* = 12.6, 6.4 Hz, 1H), 4.66 (dd, *J* = 12.6, 8.2 Hz, 1H), 4.22 (quint, *J* = 7.0 Hz, 1H), 3.48 – 3.38 (m, 2H) ppm. IR (KBr): ῡ 3064 (w, Ar-CH), 1679 (s, C=O), 1544, 1362 (s, O=N-O) cm^{-1}.

2.6. Synthesis of aza-dipyrromethene compound (3) [47]

A round bottom flask was charged with compound **2** (1.00 g, 3.29 mmol), ammonium acetate (8.88 g, 115 mmol), and *n*-butanol (10.0 mL) and heated at reflux for 48 h. During the course of the reaction, product precipitated from reaction mixture. The reaction mixture was cooled to room temperature and filtered. Isolated product was washed with cold ethanol to yield the product as a dark-blue solid, yield: 310 mg (36%). M.p. 338–340 °C. ^{1}H NMR (500 MHz, $CDCl_3$): δ = 7.98 (d, *J* = 8.4 Hz, 4H), 7.96 (d, *J* = 7.9 Hz, 4H), 7.55 (t, *J* = 7.9, 7.2 Hz, 4H), 7.49 (m, 2H), 7.41 (d, *J* = 8.4 Hz, 4H), 7.19 (s, 2H) ppm. IR (KBr): $\bar{\upsilon}$ 3260 (w, NH), 3060(w, Ar-CH), 1594 (s, C=C), 1240 (m, C-N) cm^{-1}. UV-Vis (CH_2Cl_2): λ_{max} 600 nm

2.7. Synthesis of aza-BODIPY compound (4) [47]

Compound **3** (100 mg, 193 μmol) in dichloromethane was treated with *N*,*N*-diisopropylethylamine (350 μL, 2.01 mmol) and stirred for 1 h at room temperature under N_2 atmosphere. Then, the reaction mixture was cooled down to 0^{o}C and boron triflouride diethyl etherate (870 μL, 8.68 mmol) was added and it was stirred at room temperature under N_2 atmosphere for 24 h. Then the mixture was washed with water (3×100 mL), the organic layer was dried over sodium sulphate and evaporated to dryness. Purification by column chromatography on silica eluting first with *n*-hexane/ dichloromethane (5:1) and then with *n*-pentane/chloroform (3:5) afforded target aza-BODIPY, yield: 86.2 mg (79%); m.p. 249 °C. ^{1}H NMR (500 MHz, $CDCl_3$): δ = 8.04 – 8.02 (m, 4H), 7.98 (d, *J* = 8.7 Hz, 4H), 7.50 – 7.49 (m, 6H), 7.46-7.45 (d, *J* = 8.7 Hz, 4H), 7.02 (s, 2H) ppm. ^{13}C NMR (126 MHz, $CDCl_3$): δ = 159.9, 145.4, 142.8, 135.8, 131.3, 131.1, 130.6, 130.4, 129.6, 128.9, 128.6, 119.2 ppm. ^{11}B NMR (160 MHz, $CDCl_3$): δ = 1.08, 0.88, 0.68 ppm. ^{19}F NMR (470 MHz, $CDCl_3$): δ = -131.36, -131.43, -131.49, -131.56 ppm. IR (KBr): ῡ 3059 (w, Ar-CH), 1592 (s, C=C), 1480 (m, B-N), 1110 (m, B-F), cm^{-1} HRMS: *m/z* calcd. for $[M]^+$ 566.240; found 566.652.

2.8. Synthesis of core-brominated aza-BODIPY compound (5)

To a solution of aza-BODIPY **4** (150 mg, 265 μmol) in dichloromethane (15 mL), Br_2 (43.1 μL) in dichloromethane (5.00 mL) was added dropwise at room temperature. The reaction mixture was stirred at room temperature for 6 h. Solvent was evaporated and the residue was purified by column chromatography on silica gel eluting with petroleum ether/ dichloromethane (1:1), yield: 163 mg (85%). m.p. 275 °C. ^{1}H NMR (500 MHz, $CDCl_3$): δ = 7.81 (d, *J* = 8.5 Hz, 4H), 7.71 (d, *J* = 7.0 Hz, 4H), 7.50 – 7.47 (m, 6H), 7.45 (d, *J* = 8.5 Hz, 4H) ppm. ^{13}C NMR (126 MHz, $CDCl_3$): δ = 158.7, 144.1, 143.6, 136.1, 131.8, 131.1, 130.2, 129.1, 128.9, 128.4, 128.1, 110.6 ppm. ^{11}B NMR (160 MHz, $CDCl_3$): δ = 0.29, 0.11, -0.06 ppm. ^{19}F NMR (470 MHz, $CDCl_3$): δ = -131.98, -132.04, -132.11, -132.17 ppm. IR (KBr): ῡ 3060 (w, Ar-CH), 1590 (s,C=C), 1466 (m, B-N), 1128 (m, B-F), 692 (m, C-Br) cm^{-1}

2.9. Synthesis of aza-BODIPY dimer (6)

To a solution of compound **4** (50.0 mg, 83.0 μmol) in dichloromethane (20 mL), anhydrous $FeCl_3$ (65.0 mg, 400 μmol) was added. The reaction mixture was stirred for 30 min at room temperature to perform oxidative dimerization. Then, nitrogen-flashed H_2O (40 mL) was added to the mixture and it was stirred for additional 1 h. The organic phase is washed with H_2O (2 x 50 mL), dried over Na_2SO_4, and concentrated to dryness on a rotary evaporator. The solid residue was purified by column chromatography on silica gel eluting fist with petroleum ether/ dichloromethane (1:1), then with n-hexane/chloroform (2:1), and then by preparative thin layer chromatography on silica gel eluting with n-hexane/EtOAc (3:1) to afford the product as a dark blue solid, yield: 6.10 mg (13%). mp. 379 °C. ^{1}H NMR (500 MHz, $CDCl_3$): δ = 8.11 – 8.06 (m, 4H), 7.92 (d, J = 8.6 Hz, 2H), 7.87 (d, J = 8.6 Hz, 2H), 7.58 – 7.52 (m, 6H), 7.43 – 7.39 (m, 6H), 7.33 – 7.27 (m, 8H), 7.19 – 7.17 (m, 4H), 7.07 (d, J = 8.4 Hz, 2H),

7.03 (d, J = 8.8 Hz, 4H) ppm. ^{11}B NMR (160 MHz, $CDCl_3$): δ = 1.17 (dd, J = 37, 22 Hz, 2×BF_2) ppm. ^{19}F NMR (470 MHz, CDCl3): δ = -122.10 (m), -127.79 (m), -145.05 (m), -147.74 (m) ppm. IR (KBr): ῡ 3050 (w, Ar-CH), 1594 (s,C=C), 1468 (m, B-N), 1124 (m, B-F), 694 (m, C-Cl) cm^{-1} MS (ESI+): m/z calcd for $C_{64}H_{38}Cl_4N_6Na_4$ $[M-2BF_2+4\ Na]^{+2}$ 1124.808; found 1124.4262.

3. Results and Discussion

3.1. Synthesis and Characterization

The synthetic route followed for preparation the target aza-BODIPY compounds is given in Scheme 1. Aza-BODIPY derivative carrying Cl atoms at the para positions of distal phenyl groups (**4**) was prepared to elucidate the effect of halogen atoms on photophysical properties of the aza-BODIPY dye according to a reported method with some modifications [47]. The aza-BODIPY dye **4** was prepared in an easy four step route starting from chalcone, 3-(4-chlorophenyl)-1-phenylprop-2-en-1-one **(1).** Compound **1** prepared through the aldol condensation reaction between 4-chloro benzaldehyde and acetophenone in 76 % yield.

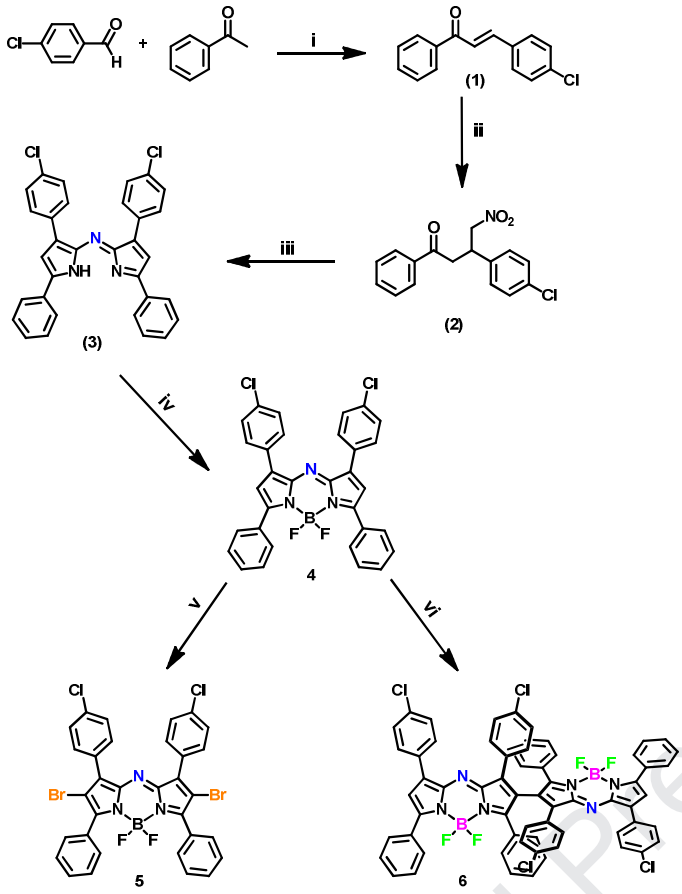

Scheme 1. Synthesis of aza-BODIPY derivatives **4**, **5** and **6**. i) EtOH, NaOH ii) EtOH, CH_3NO_2, DEA iii) CH_3COONH_4, n-BuOH iv) $BF_3.OEt_2$, DIEA, DCM v) DCM, Br_2 vi) DCM, $FeCl_3$

Michael addition reaction between **1** and nitromethane in ethanol in the presence of diethylamine as a base yielded 3-(4-dimethylaminophenyl)-4-nitro-1-phenylbutan-1-one **(2)** in 84 % yield which after heating with ammonium acetate in n-butanol at reflux for 48 hours gave dark-blue colored aza-dipyrromethene derivative **3** in 36 % yield. Aza-dipyrromethene **3** was subsequently converted into the target aza-BODIPY derivative **4** (black-yellow silvery colored compound with 79% yield) by stirring dipyrromethene compound **3** with boron triflouride diethyl etherate using diisopropylethylamine (*i*-Pr_2EtN) as a base in dichloromethane at room temperature for 24 h. With the goal of investigating the internal heavy atom effect, bromine atoms were introduced at the free β-position of both pyrrole rings

of **4** as the pyrrole ring is very reactive to electrophilic aromatic substitution. Core-brominated aza-BODIPY derivative (**5)** (85% yield) was readily obtained as deep-purple solid by reacting **4** with bromine in dichloromethane at room temperature.

There is a limited number of study on the dimeric BODIPY molecules in which the monomers are attached directly to each other without any spacer. One of them revealed a red shift in UV-Vis spectra and an advanced singlet oxygen generation efficiency compared to that of its monomers [39]. The only paper on the synthesis of homonuclear aza-BODIPY dimer demostrated that the molecule showed enhanced electronic interactions and bathochromic shift toward near-infrared region [45]. Hence, aza-BODIPY dimer was designed and synthesized through the oxidative homo-coupling of **4** in the presence of $FeCl_3$. The target compound was obtained as a dark green solid after purification by column chromatography on silica gel followed by preparative thin layer chromatography in 13% yield.

Characterization of the structures was conducted by using UV-Vis, Fluorescence, NMR (^{1}H, ^{13}C, ^{11}B and ^{19}F), and Mass and X-Ray spectroscopy techniques. The spectroscopic data of the compounds **1-6** confirmed the proposed structures. The IR spectrum of compound **3** clearly evidences the formation of aimed dipyrromethene structure by a characteristic NH stretching band at 3260 cm^{-1} and the disappearance of the NO_2 stretching bands at 1362 cm^{-1} and 1544 cm^{-1} due to symmetric and asymmetric stretching modes of the group.

In the ^{1}H NMR spectrum of **3** taken in $CDCl_3$, aromatic proton peaks appeared at 7.98-7.94, 7.57-7.53, 7.49-7.45 and 7.41-7.40 ppm as quartet, triplet, multiplet and doublet, respectively, while the pyrrolic protons came out at 7.19 ppm as a singlet peak, as expected. The ^{13}C NMR of **3** could not be obtained due to low solubility of the molecule in $CDCl_3$.

The disappearance of the characteristic NH stretching band and presence of B-N and B-F stretching bands at 1480 and 1110 cm^{-1} in the FT-IR spectrum of aza-BODIPY **4** indicated the successful complexation of **3** with boron trifloride diethyl etherate. The ^{1}H-NMR of

compound **4** in $CDCl_3$ also confirmed the proposed structure. In the ^1H NMR spectrum of **4**, aromatic protons nearest to the electronegative chlorine atoms of the distal phenyl groups were observed at 7.99-7.97 ppm as a doublet, the others appeared at 7.46-7.45 ppm as doublets with a roof effect. On the other hand, protons of the proximal phenyl units which are the ones nearest to the core were shown at 8.04-8.02 ppm because of the inductive effect in there these protons were more deshielded than the other proximal aromatic protons that were observed as a multiple peak at 7.50-7.49 ppm. Furthermore; the peak of pyrrolic protons was shifted upfield (7.02 ppm) compared to that of dipyrromethene **3** (7.19 ppm). The proposed aza-BODIPY structure was also confirmed clearly by the presence of the characteristic molecular ion peaks at m/z = 566.652 $[M]^+$ in the mass spectrum. ^{11}B spectrum of **4** exhibited a peak at 0.88 ppm confirming the presence of tetra coordinated boron atom as expected [48, 49]. The successful chealation with BF_2^+ was evidenced also by ^{19}F NMR spectroscopy with signals at δ = -131.36, -131.43, -131.49, and -131.56 ppm [50].

In the FT-IR spectrum of core-brominated aza-BODIPY **5**, the B-N, B-F, and C-Br stretching vibrations were observed at 1466, 1128, and 692 cm^{-1}, respectively. In the ^1H NMR spectrum of **5** taken in $CDCl_3$, aromatic protons of the distal phenyl groups nearest to the electronegative chlorine atoms appeared at 7.82-7.81 ppm as they were more deshielded due to the inductive effect of the halogens compared to other two protons on the ring which were observed at 7.46-7.44 ppm as doublets with a roof effect. The aromatic protons of the proximal phenyl units which are the nearest protons to the core therefore to electronegative bromine atoms, were more deshielded due to the inductive effect in there and their signal came out at 7.72-7.71 ppm, while the other protons of proximal phenyl groups were observed at 7.50-7.47 ppm. The ^{11}B NMR of **5** showed peaks at 0.29, 0.11, and -0.06 ppm indicating the presence of tetracoordinated boron atom. ^{19}F NMR spectrum of **5**, the peaks at -131.98,-132.04, -132.11,-132.17 ppm are seen due to the coupling of fluorine atom with ^{11}B atom.

Contrary to the ^{1}H NMR spectrum of **4** having four sets of aromatic protons and one pyrrolic proton, the protons of dimeric aza-BODIPY **6** were observed as eight sets at 8.11 – 8.06, 7.93-7.91, 7.87-7.85, 7.58 – 7.52, 7.42 – 7.39, 7.32 – 7.26, 7.19 – 7.17, 7.07-7.02 ppm as a multiplet, doublet, doublet, multiplet, multiplet, multiplet, multiplet, multiplet, respectively, indicating the unsymmetrical nature of dimeric aza-BODIPY. The ^{11}B NMR of **6** involved a doublet of doublet peak at 1.17 ppm while in the ^{19}F NMR spectrum displayed four multiplets at -122.10, -127.79, -145.05, -147.74 ppm owing to the inequivalence of the four fluorine atoms in the two BF_2 units [45, 50, 51]. The presence of the peaks at m/z = 1124.4262 $[M-2BF_2+4Na]^{+2}$ in the mass spectrum of aza-BODIPY dimer corresponding to decomposition products also confirmed the proposed dimeric aza-BODIPY structure such as the peak at 927 can be attributed to [M-2BF_2-3 Cl]; the peak at 991 is for [M-4 Cl] and the one at 1049 is for $[M-BF_2-Cl]^{-}$ [50, 52, 53].

Aza-BODIPY 4 carrying chlorine atom at the para position of the distal phenyl groups and its brominated analogue 5 exhibited high solubility in THF, CH_2Cl_2, $CHCl_3$ and DMSO while the aza-dipyrromethene derivative **3** is slightly soluble in $CHCl_3$ and DMSO. The solubility of dimer is relatively low when compared to those of 4 and 5. Altough the intra and inter hydrogen bonding presence in **5** revealed by X-Ray analysis, the solubility of this aza-BODIPY is high in common solvents. This can be explained by the incorporation of BF_2^{+} group into the structure and the existence of bromine atoms. Dimeric derivative **6** is soluble in THF and slightly soluble in $CHCl_3$. The relatively low solubility of the dimer could emerge from high intermolecular π-π interactions or enlarged surfaced of aromatic structures.

3.2. Crystal Structure

The single crystal of **5** with dimensions 0.01x0.02x0.40mm was grown by slow evaporation of chloroform solution. The crystal was mounted on a micromount and attached to a

goniometer head on a Bruker D8 VENTURE diffractometer equipped with PHOTON100 detector and measured with graphite monochromated Mo-Kα radiation (λ = 0.71073 Å) using 1.0° of Ω and ϕ rotation frames at room temperature. The structure has been solved by intrinsic method SHELXS-1997 (Sheldrick, 1997) [54] and refined by SHELXL-2014/7 (Sheldrick, 2014) [55]. Molecular drawings are generated using OLEX2. Ver. 1.2-dev [56]. Thermal ellipsoids are plotted in Figure 1. Figure 2 shows the crystal packing of the structure showing π—π interaction and hydrogen bonding and Figure 3 shows the halogen-π stacking. The Crystal data and structure refinement parametersof **5** is given in Table 1. Table S1-S3 (see supporting information) contain the selected bond lengths, bond and torsion angles for **5**. CCDC 1819243 contains the supplementary crystallographic data for **5**. Further details on crystal data, data collection, and refinements can be found on the supporting information.

5 crystallizes in a monoclinic lattice with $P2_1/c$ space group with unit cell containing 4 molecules and the whole crystal lattice is strongly stabilized by π—π stacking, halogen—π stacking and also by intra and intermolecular hydrogen bonding which facilitates the molecular packing. Although the phenyl rings do not show co-planarity with the boron-dipyrromethene core due to the large dihedral angles of all the phenyl rings attached to the aza-BODIPY (C15…C20 phenyl ring and C21…C26 ring has 70.5^o and 53^o dihedral angles with respect to the boron-dipyrromethene core) there is a parallel (face-to-face) π—π stacking occurring between all the aromatic rings with the same centroid—centroid distance of 5.58 Å (Figure 2). Besides π—π stacking, the crystal lattice contains Cl-π and Br- π stacking, forming a 2-dimensional supramolecular assembly. (Figure 3) Br2-C9…C13 centroid distance is 3.72 Å and Br2-C13 bond distance is 3.33 Å (1) showing an edge-on Br- π stacking and Cl1-C9….C13 centroid distance is 4.21 Å and Cl1-C13 distance is 3.30 Å(1) showing also an edge-on Cl- π stacking. The asymmetric unit of the molecule indicates the presence of overall half symmetry due to a 2-fold rotational axis as well as a mirror plane passing through B1-N2

of the central boron-dipyrromethene unit [57, 58]. This observation was also confirmed from the exactly similar bond parameters between one-half of the molecule with its other half. The two B-N bond lengths lie in the range of 1.532(2)-1.557(2) Å, which supports well with reported bond lengths proving the usual delocalization between electron deficient boron and electron rich nitrogen center [58-60]. The boron center has a tetrahedral geometry, coordinated to two nitrogen atoms from the azadipyrrinato chelate and two fluoride ions, with bond distances and angles similar to the other aza-BODIPYs reported in the literature [23]. There is also an intramolecular hydrogen bonding occurring between C11-H1---F1 with 2.31 Å distance and 124.8 (7) angle which is obviously much smaller than the sum of van der Waals radii for hydrogen and fluorine atoms (2.67 Å) [44]. Intermolecular hydrogen bonding exist between phenyl ring hydrogen and second fluorine atom with 2.52 Å (7) distance.(C20-H10---F2). The fluorine atoms are perpendicular to the boron-dipyrromethene core. Unexpected non-planarity of the boron-dipyrromethene core is observed due to the dihedral angle of 1.66^{o} between C5-N2-C4-C3 and C5-N2-C4-N1 planes.

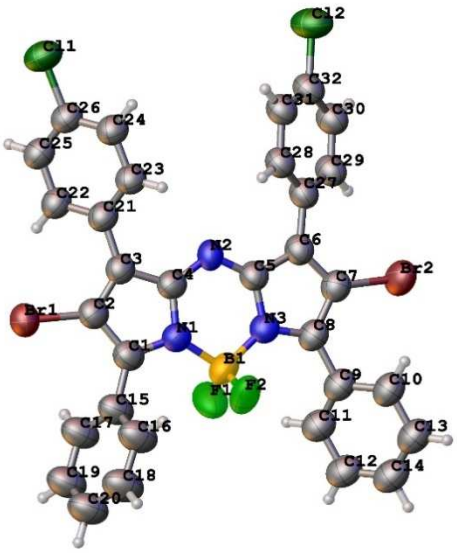

Figure 1. ORTEP drawing of **5** with atom labeling scheme. Ellipsoids are drawn at 50% probability level.

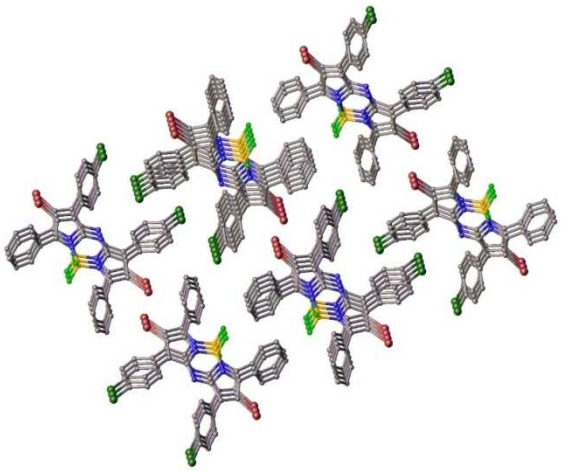

Figure 2. Crystal Packing motif of **5** showing face-to-face π stacking.

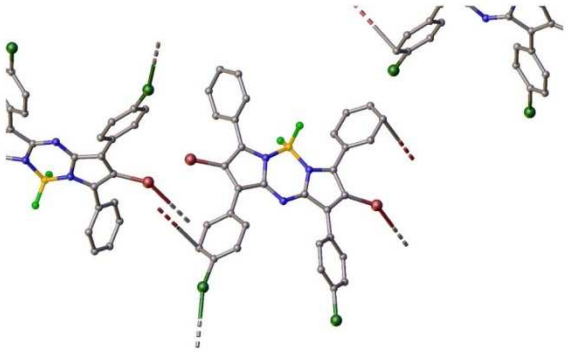

Figure 3. Crystal Packing motif of **5** showing face-to-face π stacking.

Table 1. Crystal data and structure refinement parameters of **5**

Property	5
Empirical formula	$C_{32}H_{18}BBr_2Cl_2F_2N_3$
T(K)	291(0)
λ(Å)	0.71073
Crystal system	Monoclinic
Space group	$P2_1/c$
Unit cell dimensions: (Å, º)	
a	18.032(19)
b	5.583(6)
c	28.379(3)
V(Å^3)	2850.7(5)
α	90°
β	93.83(3)
γ	90°
Z	4
Absorption coefficient (mm^{-1})	3.073
D_{calc} (g/cm^3)	1.687
F(000)	1432
Crystal size (mm)	0.01 x 0.02 x 0.40
θ range for data collection (º)	2.26 to 25.00
Index ranges	-21≤h≤20 -6≤k≤6 -32≤l≤33
Reflections collected	84210
Independent reflections	4769
Coverage of independent reflections (%)	97.3
Data/parameters	4769/380
Max. and min. transmission	1 /0.779
Final R indices [I≥2σ(I)]	R1 = 0.096 wR2 = 0.251
R indices (all data)	R1 = 0.177 wR2 = 0.333
Goodness-of-fit on F^2	1.040
Largest difference in peak and hole (e Å^{-3})	0.647/-1.286

3.3 Absorption and Fluorescence Properties

The ground state electronic absorption spectra of BODIPY compounds **A**, **4**, **5** and **6** were measured in THF (Fig. 4). Maximum absorbances of the BODIPY derivatives were observed at 650, 651, 659 and 702 nm, respectively. A THF solution of tetra-phenyl aza-BODIPY (**A**) depicted a maximum wavelength, λ_{max} at 650 nm. It was observed that the absorption

spectrum of **4** was nearly identical with that of **A** revealing that introduction of chlorine atoms onto the para positions of distal phentl groups has no significant affect on both absorption wavelength and band shape. On the other hand, direct attachment of bromine atoms at the 2,6-position of the central core caused a batochromic shift of 5 nm. This demonstrated that presence of heavy atoms on the core of aza-BODIPY structure has a higher impact on the absorption wavelength when compared with substitiutions at the para positions of the distal phenyl groups [25]. In the case of transition from monomer to dimer; absorbance maximum of dimeric aza-BODIPY **6** is red-shifted of about 50 nm when compared with aza-BODIPY **4**.

The exctintion coefficient of the investigated aza-BODIPYs were in the range of 75000-92000 $M^{-1}cm^{-1}$ which were found to be higher than those of porphyrins and chlorines [61]. These high exctition coefficients with absorptions in the therapeutic window are advantages over other PDT photosensitizers as these strong absorptions can facilitate higher singlet oxygen generations**.**

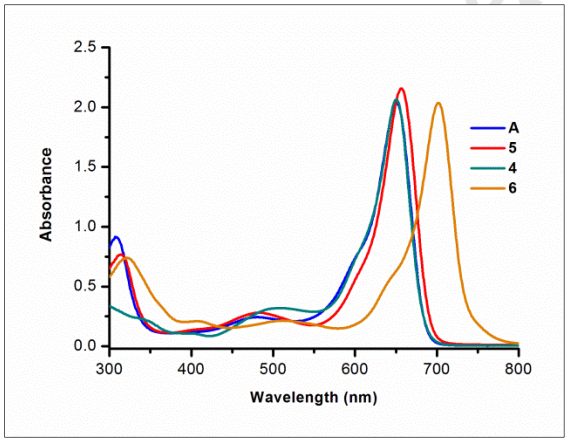

Fig 4. Absorption spectra of BODIPY derivatives **A, 4**, **5** and **6** in THF ($1x10^{-5}$ M).

Figure 5 demonstrates the fluorescence spectra of the corresponding aza-BODIPY derivatives. Excitation of aza-BODIPY derivatives in THF solution at 600 nm gave florescence spectra which were the mirror images of absorbance spectra with Stoke shifts in the range of 24-34 nm. The fluorescence emission maxima appeared at 674, 679, 684 and 736 nm for **A**, **4**, **5** and

6 respectively (Fig. 5). Florescence spectra showed a similar trend with the absorption spectra; emission wavelength of core-brominated aza-BODIPY **5** was more red-shifted than aza-BODIPY **4** carrying chlorine atoms on the distal phenyl groups. This is in alignment with literature informing that substitution at pyrrolic positions has a higher influence on the electronic structure of the BODIPY core than substitution on the phenyl ring [62]. Dimerization through the pyrrollic positions showed a high impact on the fluorescence properties; emission maximum of dimeric aza-BODIPY **6** (736 nm) showed a significant batochromic shift of 57 nm with a large Stokes shift of 34 nm when compared with its monomer **4** (679 nm). This huge red-shift may be attributed to the interactions inside a linear alignment of the same chromophores according to the exciton model of Kasha and also partially due to a higher degree of conjugation [45].

Fluorescence quantum yields (Φ_F) were determined by comparative method [63], Eq. (1)

$$\Phi_s = \Phi_{ref}\left(\frac{F_s}{F_{ref}}\right)\left(\frac{A_{ref}}{A_s}\right)\left(\frac{n_s^2}{n_{ref}^2}\right) \qquad \text{Eq. 1}$$

where F and F_{Std} are the areas under the fluorescence curves of the BODIPY derivatives (**4** to **6**) and the reference, respectively. A and A_{Std} are the absorbances of sample and reference at the excitation wavelength, and n^2 and n^2 Std are the refractive indices of solvents (*n*THF:1.407, *n*EtOH:1.361) used for the sample and the reference measurements, respectively. Fluorescein was used as a standard; =0.79 in ethanol[64]. The sample and the standard were excited at the same relevant wavelength. The solvent effect on the quantum yield was studied in THF and the emission spectra of compounds **4** to **6** in the solvent were also compared to that of the reference under the same conditions (Fig. 5). The calculated quantum yields (Φ_F) in the solvent (THF) are 0.175 for **A**, 0.162 for **4**, 0.003 for **5** and 0.100 for **6** (Table 2). Theses calculated quantum yields are all lower than the quantum yield of the

reference Fluorescein in ethanol (0.70). The chlorinated aza-BODIPY **4** did not show a remarkable decrease in fluorescence quantum yield (0.162) when compared with that of the tetra-phenyl aza-BODIPY **A** (0.175). This may be attributed to non-dominant heavy atom effect as the chlorine atoms are far away from the central core. In the case of core-brominated aza-BODIPY **5**; the lowest fluorescence quantum yield was observed indicating an efficient heavy atom effect. The fluorescence quenching of dimeric aza-BODIPY **6** was more significant than that of **4** but still higher than that of dibrominated derivative **5**. This may be caused by the possible loss of photosensitizer planarity promoting non-radiative decay to the ground state [36].

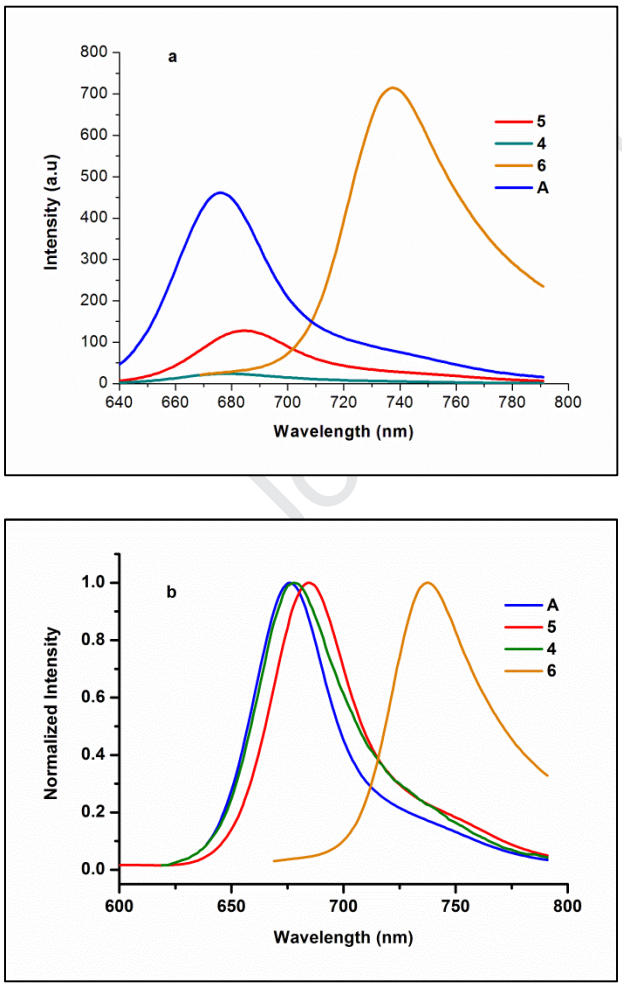

Figure 5. Emission spectra of compounds **A** to **6** in THF (**a**), Normalized Emission spectra (**b**).

Table 2. Spectral and photophysical properties of BODIPY derivatives (**A**,**4**,**5** and **6**) in THF solution

Compound	Q band λ_{max} (nm)	Emission λ_{Em} (nm)	Stoke Shifts (nm)	ε (log)	Φ_F
A	650	674	24	4.93	0.175
4	651	679	28	4.90	0.162
5	659	684	25	4.96	0.003
6	702	736	34	4.88	0.100

3.4. Quantification of singlet oxygen generation

Photodynamic therapy (PDT) is a novel method for cancer treatment based on destroying the cancer cells by singlet oxygen generated during a photocatalytic reaction. Enhanced spin-orbit perturbations is vital for an effective PDT photosensitizer because energy is transferred from the photosensitizer to the ground state oxygen in the final step of singlet oxygen generation [36]. In order to investigate their potential use as a photosensitizer in PDT; a comparative study of singlet oxygen production in THF was conducted to research the abilitiy of aza-BODIPY derivatives **4, 5** and **6** to produce singlet oxygen. The singlet oxygen generation capabilities of prepared aza-BODIPYs were determined using DPBF as a quencher of singlet oxygen in THF [65]. When the absorption band of DPBF at 416 nm reduced by light irradiation, no significant changes on the absorption bands of BODPIY derivatives in THF solutions were seen (Fig. 6 as an example for **6**). A negligible singlet oxygen generation for the aza-BODIPY derivative carrying chlorine atom at the para position of the distal phenyl ring was obtained. Substitution of chloro atoms on aryl groups did not enhance the singlet oxygen generation. In contrast; core substitiution had a significant effect on the efficiency of singlet oxygen generation, dibrominated aza-BODIPY showed the highest singlet oxygen production

among the investigated aza-BODIPY compounds. This indicated that attaching heavy atoms at the central core is an appropriate way to produce singlet oxygen (Fig. 7).

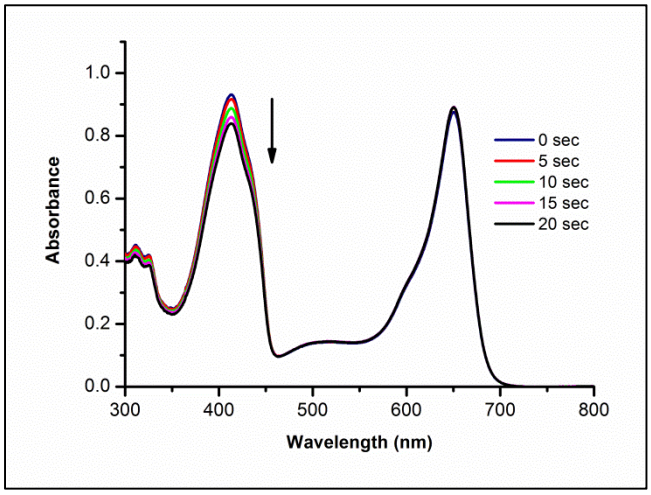

Figure 6. Electronic absorption spectral changes for compound **5** during the determination of singlet oxygen quantum yield in THF.

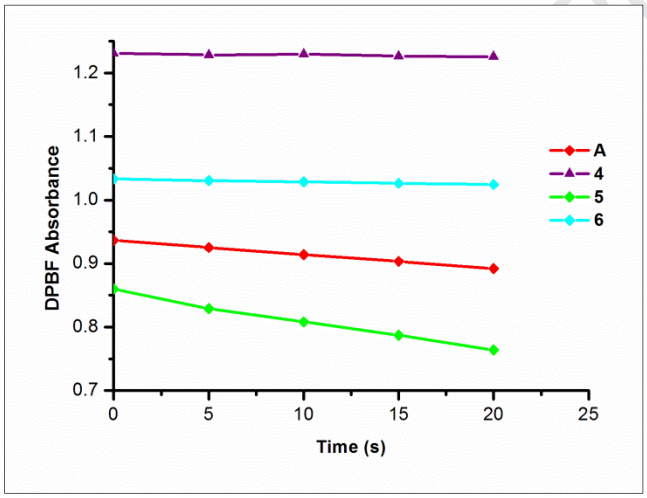

Figure 7. Decrease in the absorbance of the singlet oxygen trap DPBF molecule at 417 nm in THF for BODIPY derivatives (**A** to **6**).

4. Conclusions

In conclusion, aza-BODIPY derivative 4, 5 and 6 were prepared to investigate the influence of heavy atom effect and dimerization on the photophysical properties of aza-BODIPYs. In order to investigate the external heavy atom effect, the aza-BODIPY derivative substituted

with chlorine atoms on the para-position of distal phenyl groups (**4**) was prepared by following a reported procedure with some modifications. Bromination at the free β-positions of **4** with bromine in dichloromethane yielded core-brominated aza-BODIPY (**5**) that was used to establish the internal heavy atom effect on the photophysical properties. To evaluate dimerization effect on the photophysical properties of aza-BODIPY dyes, dimeric aza-BODIPY (**6**) was prepared by a homo-coupling reaction using $FeCl_3$ as an oxidizing agent. All of the compounds except for **4** are novel and their chemical structures are elucidated by using UV-Vis, Fluorescence, IR, NMR (^{1}H, ^{13}C, ^{11}B and ^{19}F), and MS and X-Ray spectral data. X-Ray analysis of **5** revealed a crystal lattice with π—π stacking and halogen—π stacking that form a 2-dimensional supramolecular assembly. Beside these stackings, the crystal latice is also strongly stabilized by intra and intermolecular hydrogen bonding. The presence of hydrogen bonding did not show a significant effect on the solubility of aza-BODIPY **5**.

Photophysicochemical properties of the aza-BODIPY derivatives were also investigated to examine their fluorescence behaviors and singlet oxygen generation abilities and compared with those of tetra-phenyl aza-BODIPY **A**. The absorption spectra of BODIPY compounds in THF revealed that direct attachment of bromine atoms at central core has a higher impact on the absorption wavelength when compared with substitiutions at the para positions of the distal phenyl groups. Dimerization caused a significant batochromic shift in the absorbance maximum of about 50 nm when compared with that of monomeric aza-BODIPY **4**. Emission wavelength of core-brominated aza-BODIPY **5** was more red-shifted than aza-BODIPY **4** informing that substitution at pyrrolic positions has a higher influence on the electronic structure of the BODIPY core than substitution on the phenyl ring. Dimerization through the pyrrollic positions showed a high impact on the fluorescence properties; emission maximum of dimeric aza-BODIPY **6** showed a significant batochromic shift of 57 nm with a large

Stokes shift of 34 nm when compared with its monomer **4**. The fluorescence quenching of dimeric aza-BODIPY **6** was more significant than that of **4** but still higher than that of dibrominated derivative **5** indicating an efficient heavy atom effect. As a conclusion, the newly synthesized compounds particularly the brominated derivative (**5**) having a high extinction coefficient with a strong absorption in the therapeutic window can be evaluated as a photosensitizer for photodynamic therapy applications via type II mechanism.

Acknowledgments

This work was supported by the Research Fund of Istanbul Technical University. AG thanks Turkish Academy of Sciences (TUBA) for partial support.

References

1 Gawale, Y.; Adarsh, N.; Kalva, S. K.; Joseph, J.; Pramanik, M.; Ramaiah, D.; Sekar, N. *Chemistry-a European Journal* **2017**, *23*, 6570.
2 Jiang, X. D.; Li, S.; Le Guennic, B.; Jacquemin, D.; Escudero, D.; Xiao, L. J. *Physical Chemistry Chemical Physics* **2016**, *18*, 32686.
3 Adarsh, N.; Avirah, R. R.; Ramaiah, D. *Organic Letters* **2011**, *13*, 2146.
4 Karatay, A.; Miser, M. C.; Cui, X. N.; Kucukoz, B.; Yilmaz, H.; Sevinc, G.; Akhuseyin, E.; Wu, X. T.; Hayvali, M.; Yaglioglu, H. G.; Zhao, J. Z.; Elmali, A. *Dyes and Pigments* **2015**, *122*, 286.
5 Koziar, J. C.; Cowan, D. O. *Accounts of Chemical Research* **1978**, *11*, 334.
6 McGlynn, S. P.; Reynolds, M. J.; Daigre, G. W.; Christodoyleas, N. D. *The Journal of Physical Chemistry* **1962**, *66*, 2499.
7 Sternberg, E. D.; Dolphin, D.; Bruckner, C. *Tetrahedron* **1998**, *54*, 4151.
8 Nyman, E. S.; Hynninen, P. H. *Journal of Photochemistry and Photobiology B-Biology* **2004**, *73*, 1.
9 Kamkaew, A.; Lim, S. H.; Lee, H. B.; Kiew, L. V.; Chung, L. Y.; Burgess, K. *Chemical Society Reviews* **2013**, *42*, 77.
10 Bessette, A.; Hanan, G. S. *Chemical Society Reviews* **2014**, *43*, 3342.
11 Misra, R.; Jadhav, T.; Dhokale, B.; Gautam, P.; Sharma, R.; Maragani, R.; Mobin, S. M. *Dalton Transactions* **2014**, *43*, 13076.
12 Yogo, T.; Urano, Y.; Ishitsuka, Y.; Maniwa, F.; Nagano, T. *Journal of the American Chemical Society* **2005**, *127*, 12162.
13 Kolemen, S.; Akkaya, E. U. *Coordination Chemistry Reviews* **2018**, *354*, 121.
14 Bucher, L.; Desbois, N.; Harvey, P. D.; Sharma, G. D.; Gros, C. P. *Solar Rrl* **2017**, *1*.
15 Zhao, J. Z.; Xu, K. J.; Yang, W. B.; Wang, Z. J.; Zhong, F. F. *Chemical Society Reviews* **2015**, *44*, 8904.

16 Durantini, A. M.; Heredia, D. A.; Durantini, J. E.; Durantini, E. N. *European Journal of Medicinal Chemistry* **2018**, *144*, 651.
17 Wu, D.; Chen, L.; Lee, W.; Ko, G.; Yin, J.; Yoon, J. *Coordination Chemistry Reviews* **2018**, *354*, 74.
18 Klfout, H.; Stewart, A.; Elkhalifa, M.; He, H. S. *Acs Applied Materials & Interfaces* **2017**, *9*, 39873.
19 Squeo, B. M.; Gregoriou, V. G.; Avgeropoulos, A.; Baysec, S.; Allard, S.; Scherf, U.; Chochos, C. L. *Progress in Polymer Science* **2017**, *71*, 26.
20 Lakshmi, V.; Rao, M. R.; Ravikanth, M. *Organic & Biomolecular Chemistry* **2015**, *13*, 2501.
21 Kumar, S.; Khan, T. K.; Ravikanth, M. *Tetrahedron* **2015**, *71*, 7608.
22 Agostinis, P.; Berg, K.; Cengel, K. A.; Foster, T. H.; Girotti, A. W.; Gollnick, S. O.; Hahn, S. M.; Hamblin, M. R.; Juzeniene, A.; Kessel, D.; Korbelik, M.; Moan, J.; Mroz, P.; Nowis, D.; Piette, J.; Wilson, B. C.; Golab, J. *Ca-a Cancer Journal for Clinicians* **2011**, *61*, 250.
23 Killoran, J.; Allen, L.; Gallagher, J. F.; Gallagher, W. M.; O'Shea, D. F. *Chemical Communications* **2002**, 1862.
24 Aksenova, I. V.; Kuznetsova, R. T.; Pozdnyakov, I. P.; Plyusnin, V. F.; Berezin, M. B.; Bumagina, N. A.; Jarnikova, E. S.; Parkhats, M. V.; Dzhagarov, B. M. *Journal of Photochemistry and Photobiology a-Chemistry* **2017**, *344*, 206.
25 Adarsh, N.; Shanmugasundaram, M.; Avirah, R. R.; Ramaiah, D. *Chemistry-a European Journal* **2012**, *18*, 12655.
26 Partyka, D. V.; Deligonul, N.; Washington, M. P.; Gray, T. G. *Organometallics* **2009**, *28*, 5837.
27 Yakubovskyi, V. P.; Shandura, M. P.; Kovtun, Y. P. *Synthetic Communications* **2010**, *40*, 944.
28 Gawale, Y.; Mangalath, S.; Adarsh, N.; Joseph, J.; Ramaiah, D.; Sekar, N. *Dyes and Pigments* **2019**, *171*, 107684.
29 Staudinger, C.; Breininger, J.; Klimant, I.; Borisov, S. M. *Analyst* **2019**, *144*, 2393.
30 Karlsson, J. K. G.; Harriman, A. *Journal of Physical Chemistry A* **2016**, *120*, 2537.
31 Xu, Y.; Zhao, M.; Zou, L.; Wu, L.; Xie, M.; Yang, T.; Liu, S.; Huang, W.; Zhao, Q. *ACS Applied Materials & Interfaces* **2018**, *10*, 44324.
32 Adarsh, N.; Babu, P. S. S.; Avirah, R. R.; Viji, M.; Nair, S. A.; Ramaiah, D. *Journal of Materials Chemistry B* **2019**, *7*, 2372.
33 Jiang, X.; Zhang, T.; Sun, C.; Meng, Y.; Xiao, L. *Chinese Chemical Letters* **2019**, *30*, 1055.
34 Ortiz, M. J.; Agarrabeitia, A. R.; Duran-Sampedro, G.; Prieto, J. B.; Lopez, T. A.; Massad, W. A.; Montejano, H. A.; Garcia, N. A.; Arbeloa, I. L. *Tetrahedron* **2012**, *68*, 1153.
35 Sauerwein, B.; Schuster, G. B. *Journal of Physical Chemistry* **1991**, *95*, 1903.
36 Gorman, A.; Killoran, J.; O'Shea, C.; Kenna, T.; Gallagher, W. M.; O'Shea, D. F. *Journal of the American Chemical Society* **2004**, *126*, 10619.
37 Awuah, S. G.; Polreis, J.; Biradar, V.; You, Y. *Organic Letters* **2011**, *13*, 3884.
38 Loudet, A.; Burgess, K. *Chemical Reviews* **2007**, *107*, 4891.
39 Zhang, X. F. *Journal of Photochemistry and Photobiology a-Chemistry* **2018**, *355*, 431.
40 Shimizu, S.; Murayama, A.; Haruyama, T.; Iino, T.; Mori, S.; Furuta, H.; Kobayashi, N. *Chemistry-a European Journal* **2015**, *21*, 12996.
41 Shimizu, S.; Iino, T.; Saeki, A.; Seki, S.; Kobayashi, N. *Chemistry-a European Journal* **2015**, *21*, 2893.

42 Shimizu, S.; Iino, T.; Araki, Y.; Kobayashi, N. *Chemical Communications* **2013**, *49*, 1621.
43 Tamada, M.; Iino, T.; Wang, Y. M.; Ide, M.; Saeki, A.; Furuta, H.; Kobayashi, N.; Shimizu, S. *Tetrahedron Letters* **2017**, *58*, 3151.
44 Wang, Y. F.; Chen, L.; El-Shishtawy, R. M.; Aziz, S. G.; Mullen, K. *Chemical Communications* **2014**, *50*, 11540.
45 Nepomnyashchii, A. B.; Broring, M.; Ahrens, J.; Bard, A. J. *Journal of the American Chemical Society* **2011**, *133*, 8633.
46 Loudet, A.; Bandichhor, R.; Wu, L. X.; Burgess, K. *Tetrahedron* **2008**, *64*, 3642.
47 Li, C. H.; Shen, T. H.; Chen, X. L.; Zhou, C. Q.; Zhang, C.; Song, Q. B. *Chinese Journal of Organic Chemistry* **2011**, *31*, 1440.
48 Ozcelik, S.; Karaoglan, G. K.; Gumrukcu, G.; Erdogmus, A.; Gul, A. *Journal of Organometallic Chemistry* **2014**, *769*, 17.
49 Ozcelik, S.; Gul, A. *Journal of Organometallic Chemistry* **2012**, *699*, 87.
50 Taguchi, D.; Nakamura, T.; Horiuchi, H.; Saikawa, M.; Nabeshima, T. *Journal of Organic Chemistry* **2018**, *83*, 5331.
51 Alamiry, M. A. H.; Benniston, A. C.; Hagon, J.; Winstanley, T. P. L.; Lemmetyinen, H.; Tkachenko, N. V. *Rsc Advances* **2012**, *2*, 4944.
52 Swamy, C. A.; Priyanka, R. N.; Mukherjee, S.; Thilagar, P. *European Journal of Inorganic Chemistry* **2015**, 2338.
53 Wang, D. G.; Song, F.; Tang, H.; Jia, X. R.; Song, M.; Kuang, G. C. *New Journal of Chemistry* **2017**, *41*, 5263.
54 Sheldrick, G. M. *Acta Crystallographica Section A* **2008**, *64*, 112.
55 Sheldrick, G. M. In *SHELXS97 and SHELXL97. Program for Crystal Structure Solution and Refinement*; SHELXS97 and SHELXL97. Program for Crystal Structure Solution and Refinement, University of Göttingen, Göttingen, 1997.
56 Dolomanov, O. V.; Bourhis, L. J.; Gildea, R. J.; Howard, J. A. K.; Puschmann, H. *Journal of Applied Crystallography* **2009**, *42*, 339.
57 Kumar, S.; Gobeze, H. B.; Chatterjee, T.; D'Souza, F.; Ravikanth, M. *The Journal of Physical Chemistry A* **2015**, *119*, 8338.
58 Mazel, A.; Baudron, S. A.; Hosseini, M. W. *Crystengcomm* **2017**, *19*, 897.
59 Kumar, S.; Thorat, K. G.; Ravikanth, M. *The Journal of Organic Chemistry* **2017**, *82*, 6568.
60 Chen, J. J.; Conron, S. M.; Erwin, P.; Dimitriou, M.; McAlahney, K.; Thompson, M. E. *Acs Applied Materials & Interfaces* **2015**, *7*, 662.
61 Sharman, W. M.; Allen, C. M.; van Lier, J. E. *Drug Discovery Today* **1999**, *4*, 507.
62 Koksoy, B.; Kaya, E. N.; Hacivelioglu, F.; Yesilot, S.; Durmus, M. *Dyes and Pigments* **2017**, *140*, 384.
63 Sen, P.; Atmaca, G. Y.; Erdogmus, A.; Dege, N.; Genc, H.; Atalay, Y.; Yildiz, S. Z. *Journal of Fluorescence* **2015**, *25*, 1225.
64 Sen, P.; Yildiz, S. Z.; Atalay, Y.; Dege, N.; Demirtas, G. *Journal of Luminescence* **2014**, *149*, 297.
65 Gunsel, A.; Guzel, E.; Bilgicli, A. T.; Atmaca, G. Y.; Erdogmus, A.; Yarasir, M. N. *Journal of Luminescence* **2017**, *192*, 888.

Research Highlights

- Aza-BODIPY derivatives with chlorine atoms on the para-position of the distal phenyl groups and its core-brominated analogue were prepared.
- Novel dimeric aza-BODIPY was prepared through oxidative homocoupling with $FeCl_3$.
- The effects of incorporation of halogen atoms at different positions and dimerization on their photophysical properties were investigated.
- The aza-BODIPY derivative carrying bromine atoms at the central core displayed the utmost efficiency for singlet oxygen generation.